Heredity

ORIGINAL ARTICLE

Transgressive physiological and transcriptomic responses to light stress in allopolyploid *Glycine dolichocarpa* (Leguminosae)

JE Coate, AF Powell, TG Owens and JJ Doyle

Allopolyploidy is often associated with increased photosynthetic capacity as well as enhanced stress tolerance. Excess light is a ubiquitous plant stress associated with photosynthetic light harvesting. We show that under chronic excess light, the capacity for non-photochemical quenching (NPQ_{max}), a photoprotective mechanism, was higher in a recently formed natural allotetraploid (*Glycine dolichocarpa*, designated 'T2') than in its diploid progenitors (*G. tomentella*, 'D3'; and *G. syndetika*, 'D4'). This enhancement in NPQ_{max} was due to an increase in energy-dependent quenching (qE) relative to D3, combined with an increase in zeaxanthin-dependent quenching (qZ) relative to D4. To explore the genetic basis for this phenotype, we profiled D3, D4 and T2 leaf transcriptomes and found that T2 overexpressed genes of the water–water cycle relative to both diploid progenitors, as well as genes involved in cyclic electron flow around photosystem I (CEF-PSI) and the xanthophyll cycle, relative to D4. Xanthophyll pigments have critical roles in NPQ, and the water–water cycle and CEF-PSI are non-photosynthetic electron transport pathways believed to facilitate NPQ formation. In the absence of CO_2, T2 also exhibited greater quantum yield of photosystem II than either diploid, indicating a greater capacity for non-photosynthetic electron transport. We postulate that, relative to its diploid progenitors, T2 is able to achieve higher NPQ_{max} due to an increase in xanthophyll pigments coupled with enhanced electron flow through the water–water cycle and CEF-PSI.

Heredity (2013) 110, 160–170; doi:10.1038/hdy.2012.77; published online 14 November 2012

INTRODUCTION

All flowering plants have a history of whole genome duplication or polyploidy (Jiao *et al.*, 2011), and an estimated 15% of all angiosperm speciation events have involved polyploidy (Wood *et al.*, 2009). Polyploids often exhibit greater colonizing ability and expanded ecological tolerances and geographical ranges compared with their diploid progenitors (Lewis, 1980; Otto and Whitton, 2000; Doyle *et al.*, 2004; Ramsey, 2011). One proposed explanation for the prevalence and apparent success of polyploids in flowering plants is that they possess greater stress tolerances than their diploid progenitors, making them better adapted to extreme and/or adverse environments (Ehrendorfer, 1980; Lewis, 1980; Otto and Whitton, 2000).

During times of high and/or fluctuating light intensities, as well under stresses that impair the capacity for carbon fixation, plants routinely absorb more energy from sunlight than they can use for photosynthesis (Demmig-Adams and Adams, 2000; Avenson *et al.*, 2004). This excess absorbed light energy (hereafter referred to as excess light (EL)) can generate reactive oxygen species that damage the photosynthetic apparatus (Niyogi, 2000; Murchie and Niyogi, 2011). Thus, stress from EL is a ubiquitous and inevitable byproduct of photosynthetic light harvesting.

Photosynthesis as a whole is known to be affected by polyploidy (Warner and Edwards, 1993; Coate *et al.*, 2012). Studies involving a wide range of polyploid species, including auto- and allopolyploids in both C3 and C4 species, have shown that polyploids often have larger mesophyll cells with more chloroplasts, higher chlorophyll and rubisco contents and greater photosynthetic capacities per cell than their diploid counterparts (for example, Dunstone and Evans, 1974; Molin *et al.*, 1982; citations in Warner and Edwards, 1993; Coate *et al.*, 2012). At the whole-leaf level, the effects of polyploidy are highly variable and not all polyploids examined exhibit greater photosynthetic capacities per unit leaf area (for example, Coate *et al.*, 2012).

One aspect of photosynthesis that has not been studied in the context of polyploidy is photoprotection, the set of mechanisms by which plants avoid damage from EL. These mechanisms include avoidance of EL via leaf and/or chloroplast movement, acclimatory adjustments to the size of light harvesting antenna, constitutive and regulated thermal dissipation of EL energy, alternative sinks for the electron transport chain (for example, photorespiration, the water–water cycle) and scavenging of reactive oxygen species to prevent photooxidative damage (Niyogi, 2000; Li *et al.*, 2009; Murchie and Niyogi, 2011). Because thermal dissipation of EL energy can be measured as quenching of chlorophyll fluorescence, this component of photoprotection is also known as non-photochemical quenching (NPQ). Several strategies for NPQ are evolutionarily conserved throughout the plant kingdom (Avenson *et al.*, 2004; Horton and Ruban, 2005) and are essential for plant fitness in the field (for example, Johnson *et al.*, 1993; Kulheim *et al.*, 2002; Krah and Logan, 2010).

Department of Plant Biology, Cornell University, Ithaca, NY, USA
Correspondence: Dr JE Coate, Department of Plant Biology, Cornell University, 412 Mann Library Building, Ithaca, NY 14853, USA.
E-mail: jec73@cornell.edu

Based primarily on the kinetics of induction and relaxation, NPQ is known to consist of several distinct components (Melkonian et al., 2004; Baker, 2008; Nilkens et al., 2010), including a rapidly inducible and reversible component termed energy-dependent quenching (qE; Li et al., 2000), a component with intermediate formation and relaxation kinetics, termed qZ (Nilkens et al., 2010), and components that are either slowly reversible or completely irreversible in the dark collectively termed qI (Niyogi, 2000; Murchie and Niyogi, 2011). The irreversible component of qI results from photooxidative damage to the PSII reaction center that requires light-dependent protein synthesis for repair, but now qI is also believed to include a regulated component not involving damage to PSII (Lambrev et al., 2010; Murchie and Niyogi, 2011).

The non-damage components of NPQ are not fully understood, but qE requires the PSII subunit, PsbS (Li et al., 2000; 2002), and qE, qZ and qI all require xanthophyll cycle enzymes, including violaxanthin deepoxidase (VDE), for optimal function (Yamamoto and Kamite, 1972; Demmig-Adams et al. 1990; Szabo et al., 2005; Nilkens et al., 2010). Both PsbS and VDE require a low lumenal pH for activation (Szabo et al., 2005; Horton et al., 2008). Photosynthetic electron transport contributes H^+ to the thylakoid lumen via the Q cycle at the cytochrome b_6f complex and water splitting at PSII. Additionally, at the onset of illumination and under various stress conditions (for example, EL, low CO_2), alternative electron flows, including the water–water cycle and cyclic electron flow around photosystem I (CEF-PSI), are believed to have an important role in establishing a pH gradient and triggering NPQ (Neubauer and Yamamoto, 1992; Asada, 1999; Joliot and Joliot, 2002; Rizhsky et al., 2003; Miyake et al., 2004; Joliot and Johnson, 2011; Munekage et al., 2004; Murchie and Niyogi, 2011).

We hypothesized that an enhanced capacity for photoprotection or greater flexibility to adjust to different light environments could potentially have contributed to the success and expanded ranges of some polyploids. Glycine dolichocarpa (designated 'T2') is an allotetraploid centered in Australia that resulted from crosses between the diploid species G. tomentella ('D3') and G. syndetika ('D4') within the last 100 000 years (Doyle et al., 2004). This timeframe corresponds with major environmental changes associated with the last ice age (Hope, 1994) as well as the first human colonization of the continent (Hudjashov et al., 2007; Notaro et al., 2011) that likely increased demands on photoprotective mechanisms. Additionally, like many other polyploid species, T2 has expanded its range relative to its diploid progenitors (Doyle et al., 2002). We speculated, therefore, that allopolyploidy conferred an enhanced capacity for NPQ in T2, enabling it to become established in the presence of its diploid progenitor species, and to expand its range outside of Australia.

To test this hypothesis, we quantified and compared NPQ phenotypes (NPQ capacity, qE, qZ and qI) in T2, D3 and D4 under conditions where light intensity is either limiting to photosynthesis (limiting light (LL)) or in excess of what can be utilized for photosynthesis (EL). By quantifying NPQ under both light intensities, we tested whether (1) allopolyploidy has increased NPQ capacity in T2, and (2) if any such increase is constitutive, or if it can be modulated in response to light intensity. We show that T2 exhibited a transgressive increase in NPQ under EL but not under LL, suggesting that it has a greater capacity to respond to and protect itself from EL stress. We then profiled the limiting and EL leaf transcriptomes of each species in order to quantify global transcriptional patterns associated with enhanced NPQ and to explore the genetic basis for the observed NPQ phenotypes. Transcript profiles were consistent with T2 having a lesser overall response to EL at the level of gene expression and with T2 experiencing less photooxidative stress than either diploid progenitor under EL. Despite a smaller transcriptional response overall, T2 overexpressed genes involved in the water–water cycle, cyclic electron flow around photosystem I and the carotenoid biosynthetic pathway (including the xanthophyll cycle) under EL. We discuss how upregulation of genes in these pathways might explain the observed NPQ phenotypes.

METHODS

Plant material

The study group consisted of the natural allopolyploid, G. dolichocarpa ($2n = 80$; designated 'T2') and its diploid progenitors, G. tomentella ($2n = 40$; 'D3') and G. syndetika ($2n = 40$; 'D4'), which are perennial relatives of the cultivated soybean (G. max; Doyle et al., 2004; Pfeil et al., 2006). The two diploid species, D3 and D4, diverged approximately 3.2 MYA (Egan AN and Doyle JJ, unpublished results), and hybridized to give rise to T2 within the last 100 000 years (Doyle et al., 2004). These and other perennial Glycine species are largely selfers but show geographical and ecological variation among accessions; each accession represents a sample collected from a population (generally from a single individual) and propagated by selfing for one to two generations in Commonwealth Scientific and Industrial Research Organization (CSIRO) greenhouses. The ranges of all three species are centered in Queensland, NE Australia, and overlap (Doyle et al., 2002). D3 is also found in Papua New Guinea, and T2 is also found in Taiwan (Doyle et al., 2002). NPQ measurements were made on 3–4 accessions per species: three accessions of D3 (CSIRO accession numbers G1366, G1403 and G1820), three accessions of D4 (G1300, G2073 and G2321), and four accessions of T2 (G1134, G1188, G1393 and G1854). Transcript profiling data (RNA-Seq) were collected for the same accessions, with the exception of T2 accession G1854, for which Illumina library construction was unsuccessful. Accessions were selected to sample the geographical range of each species (Supplementary Figure S1). D3 accession, G1366, was collected in Papua New Guinea, and T2 accession, G1854, was collected in Taiwan. All remaining accessions were collected in Queensland, Australia.

For both NPQ and transcript profiling, plants were grown in a common growth chamber with a 12 h/12 h light/dark cycle, 22 °C/18 °C day/night temperature regime and a light intensity of either 125 μmol $m^{-2} s^{-1}$ (LL) or 800 μmol $m^{-2} s^{-1}$ (EL); 800 μmol $m^{-2} s^{-1}$ was chosen as the intensity for EL based on measurements of linear electron transport (ETR) that showed that all genotypes approach light saturation at 800 μmol $m^{-2} s^{-1}$ (Supplementary Figure S2).

For all experiments, the central leaflet of a trifoliolate leaf was sampled except in cases where it was damaged, in which case a lateral leaflet was used. All samples were taken from approximately 1-week-old, fully expanded leaves, and were collected 0.5–2.0 h into the light period.

Non-photochemical quenching

NPQ was measured using an FMS2 chlorophyll fluorometer (Hansatech, Norfolk, England). For each light treatment (LL and EL), NPQ measurements were made on 2–4 leaflets per individual and three individuals per accession. For each leaflet, NPQ was measured on the day of collection. The order in which leaflets collected in a given day were measured was randomized in order to reduce potentially confounding effects of diurnal variation in NPQ. All measurements for a given light treatment were collected over the course of 2 weeks, and the order in which individuals were sampled during this time was randomized. Leaflets were dark adapted on wet paper towels for ⩾15 min before measurement in order to obtain an estimate of maximal fluorescence (F_m), minimal fluorescence (F_o), variable fluorescence ($F_v = F_m - F_o$) and maximum quantum yield of photosystem II (F_v/F_m) (Maxwell and Johnson, 2000). If a leaflet was photoinhibited ($F_v/F_m < 0.8$), it was placed under low light (approximately 30 μmol $m^{-2} s^{-1}$) for 1–2 h to allow for relaxation of NPQ and PSII repair, then dark adapted again, before measurement. An estimate of F_m in the absence of any photoinhibition is required to estimate maximum NPQ (NPQ_{max}). Therefore, leaflets that were still photoinhibited after this recovery period were discarded, and only leaflets with $F_m > 0.8$ were used for NPQ measurement.

NPQ_{max} was determined by measuring maximal fluorescence under illumination (F_m') under non-photosynthetic conditions (a gas mixture of 0% CO_2 to prevent carbon fixation, 2% O_2 to enable formation of a trans-thylakoid pH gradient necessary for optimal NPQ and 98% N_2) and high light (2000 μmol m^{-2} s^{-1}; Demmig-Adams *et al.*, 2006). Fluorescence measurements were performed on detached leaflets in a chamber through which the gas mixture was continuously flowing. F_m' was measured under these conditions every 15–60 s for 12 min.

NPQ was calculated as $(F_m - F_m')/F_m'$ (Maxwell and Johnson, 2000). For each individual and time point, values from individual leaves were averaged. Curves were fitted to the averaged data (NPQ vs time) for each individual by non-linear regression using SigmaPlot (Systat Software Inc., San Jose, CA, USA). Data were fit to a two-phase model of exponential rise to a maximum:

$$NPQ = a(1 - e^{-b*x}) + c(1 - e^{-d*x})$$

This model was chosen because NPQ induction is known to involve two distinct phases, the first triggered by protonation of the PsbS protein and the second resulting from deepoxidation of violaxanthin to zeaxanthin (Horton *et al.*, 2008; Nilkens *et al.*, 2010). Coefficients of determination (R^2) between this model and the data, as calculated by SigmaPlot, were consistently higher than for single component models, and raw residuals between fitted and observed data were more randomly distributed (data not shown), indicating a better fit to the data.

The relative contributions of qE, qZ and qI to NPQ_{max} were estimated by monitoring NPQ relaxation kinetics in the dark following NPQ_{max} measurement as described (Melkonian *et al.*, 2004). Briefly, following the 12-min exposure to saturating light used to measure NPQ, leaves were left in darkness, and F_m' was re-measured after 10 min and again after 2–4 h. The qE component of NPQ relaxes within 10 min of a leaf being placed in darkness (Krause and Jahns, 2004), such that NPQ persisting after 10 min in the dark consists of qZ + qI. The qZ component of NPQ relaxes within tens of minutes (Nilkens *et al.*, 2010; Murchie and Niyogi, 2011), so that NPQ persisting after ⩾ 2 h in the dark consists of qI, which is either irreversible in the dark or requires several hours to relax (Nilkens *et al.*, 2010; Murchie and Niyogi, 2011).

Consequently, (qI + qZ) was calculated as $(F_m - F_{m1}')/F_{m1}'$, where F_{m1}' is the value of F_m' measured after 10 min in the dark following NPQ_{max} measurement. qZ was calculated as $(F_m - F_{m2}')/F_{m2}'$, where F_{m2}' is the value of F_m' measured after 2–4 h in the dark following measurement of NPQ_{max}. qE was calculated as $NPQ_{max} - (qI + qZ)$ and qI was calculated as $(qI + qZ) - qZ$. A fourth component of NPQ termed state transitions (qT) has similar relaxation kinetics to qZ but only contributes appreciably to NPQ under low light (Walters and Horton, 1991; Nilkens *et al.*, 2010), hence was not a significant component of NPQ under our measurement conditions.

With the exception of the damage component of qI, which requires light-dependent chloroplast protein synthesis for PSII repair, all NPQ components begin to relax at the outset of the dark recovery period. Thus, an absolute separation of qE, qZ and qI by our method is not possible (van Wijk and van Hasselt, (1993); Melkonian *et al.*, 2004), and there was necessarily some contribution of qZ and qI to our estimate of qE and some contribution of qI to our estimate of qZ. Our estimates of these individual components should, therefore, be taken as approximations.

Quantum yield of photosystem II

In order to quantify quantum yield of photosystem II (Φ_{PSII}) under NPQ measurement conditions, the steady state level of fluorescence during illumination (F_o') was also measured during collection of NPQ data. Φ_{PSII} was calculated as $(F_m' - F_o')/F_m'$ (Maxwell and Johnson, 2000). As with NPQ, for each individual and time point, values from individual leaves were averaged. Curves were fitted to the averaged data (Φ_{PSII} vs time) for each individual by non-linear regression using SigmaPlot. Data were fit to a one-component model of exponential rise to a maximum:

$$\Phi_{PSII} = a(1 - e^{-b*x}).$$

Accession means were averaged to estimate species means and standard deviations.

Statistical analysis—NPQ and ΦPSII

We tested for differences in NPQ_{max}, qE, qZ, qI, and Φ_{PSII} using general linear models in JMP 9.0.2 (SAS Institute, Cary, NC, USA, 2010), checking the data and residuals for normality using Shapiro–Wilk tests. Initially, we specified the general linear model to use a nominal response variable, with light treatment (LL or EL), species (D3, D4, or T2) and their interaction as fixed effects, and accession as a random effect. For NPQ_{max}, qZ, qI, and Φ_{PSII}, < 8% of total variance was attributed to accession (the random effect), and inclusion of this variable had no effect on the significance of the fixed effects. Consequently, for these response variables, we used a simpler model excluding accession as a random effect. For qE, 59% of total variance was ascribed to accession, and its inclusion in the model changed the outcome of significance tests for the fixed effects. Consequently, we kept accession as a random effect in the model for qE. For all significant effects, Tukey's HSD tests were performed to identify pairwise differences.

Transcript profiling

Leaflets were pooled from six individuals per accession (one leaflet per individual), and RNA-Seq libraries were constructed from the pooled tissue. For each light treatment, all RNA-Seq tissue was collected in a single morning and immediately frozen in liquid nitrogen. Total RNA was isolated from pooled leaf tissue using Plant RNeasy kit with on-column DNase treatment (Qiagen, Valencia, CA, USA). Single-end RNA-Seq libraries were constructed following the Illumina mRNA sequencing protocol (Illumina, San Diego, CA, USA), with the following modifications: (1) two rounds of polyA selection were performed using the Dynabeads mRNA DIRECT kit (Life Technologies, Carlsbad, CA, USA); (2) RNA was fragmented for 2 min at 70 °C using the RNA fragmentation reagents kit (Life Technologies; and (3) Illumina PE adapters were replaced with custom-made adapters containing 3nt barcodes in order to facilitate multiplexing of samples (Supplementary Table S1).

Sequencing was performed on the GAIIx platform (Illumina), generating 88nt reads. Equimolar amounts of three barcoded libraries were combined and sequenced per channel. Raw data files were imported into GenomeQuest (www.genomequest.com; GenomeQuest Inc., Westborough, MA, USA) and processed as follows. Ambiguous residues and residues with Phred quality scores < 11 were trimmed from both ends of reads. Following this step, reads were discarded that met any of the following conditions: (1) contained 10 or more residues with quality scores < 11; (2) contained ambiguous residues; or (3) were < 28 residues in length. The remaining reads were separated based on barcode sequences in the adapters.

Processed reads were then mapped against the 8x genome sequence of soybean (*Glycine max*, version Glyma1; Soybean Genome Project, DoE Joint Genome Institute; Schmutz *et al.*, 2010), which diverged from the common ancestor of D3, D4 and T2 approximately 5 MYA (Innes *et al.*, 2008), using default parameters in the GenomeQuest RNA-Seq workflow. Reads mapping equally well to more than one location in the reference genome were excluded from the analysis because their gene of origin was ambiguous.

Reads from uniquely aligned sequences were used to estimate expression levels after normalizing read counts to account for overall sample sizes. Transcript abundance per transcriptome for a given gene was estimated as the number of reads unambiguously mapped to that gene per kilobase (kb) and per million unambiguously mapped reads generated by that library (reads per kb per million reads (RPKM); Mortazavi *et al.*, 2008). For statistical analyses, the three accessions sequenced per species were treated as biological replicates for that species. Significant differences in expression (false discovery rate (FDR) < 0.05; Benjamini–Hochberg adjustment) between species were identified by DESeq, an R/Bioconductor statistical package specifically designed for use with RNA-Seq data (Anders and Huber, 2010). Pearson correlation coefficients of RPKM values were calculated for pairwise comparisons of transcriptomes using Microsoft Excel (Microsoft, Redmond, WA, USA).

RESULTS
Non-photochemical quenching
T2 has enhanced NPQ capacity under EL. Light treatment ($F_{1,14} = 10.378$, $P = 0.006$), species ($F_{2,14} = 8.124$, $P = 0.005$) and their interaction ($F_{2,14} = 7.796$, $P = 0.005$) all had significant effects on

NPQ capacity (NPQ$_{max}$). The allotetraploid (T2) and its diploid progenitors (D3 and D4) exhibited comparable NPQ$_{max}$ when grown under LL (Figures 1a and c; Supplementary Table S2). NPQ$_{max}$ was also comparable between the two diploid species under EL, with neither diploid exhibiting an increase in NPQ$_{max}$ between LL and EL. By contrast, NPQ$_{max}$ increased significantly in T2 from LL to EL and was significantly higher in T2E than in D4E or D3E (Figures 1b and c; Supplementary Table S2).

T2 differs from D3 and D4 in the contributions of qE, qZ and qI to NPQ. By monitoring the relaxation kinetics of NPQ in the dark, we dissected NPQ$_{max}$ into its component parts: energy-dependent quenching (qE), zeaxanthin-dependent quenching (qZ) and photo-inhibition (qI). Under LL, we observed no differences between D3, D4 and T2 in the contributions of these individual components to NPQ$_{max}$ (Figure 2; Supplementary Table S2). As has been observed in other species (Niyogi *et al.*, 2005; Szabo *et al.*, 2005), qE was the major component (71–80%) of NPQ in D3, D4 and T2. qZ comprised the next largest portion (12–18%), and qI was the smallest portion (8–11%) of total NPQ in all the three species (Figure 2; Supplementary Table S2).

Under EL, the fraction of NPQ$_{max}$ contributed by qE decreased in all the three species, though the difference was only significant in D3 (Figure 2). T2 had the smallest decrease in qE between LL and EL, and as a result qE was significantly higher in T2 than in D3 (but not in D4) under EL. Conversely, qZ increased in EL relative to LL in all the three species, though the increase was not significant in D4. The increase was greatest in T2 and smallest in D4 (Figure 2; Supplementary Table S2). As a result, qZ was significantly higher in T2 than in D4, but not in D3, under EL. No significant differences were detected in qI, though this component of NPQ was numerically lower in T2 than in either diploid under EL (Figure 2; Supplementary Table S2). Thus, the high NPQ$_{max}$ phenotype in T2 was due primarily to greater qE relative to D3 and greater qZ relative to D4.

Transcript profiling

In order to compare gene expression responses with EL, and to explore the genetic basis for the observed differences in NPQ, we profiled the LL and EL leaf transcriptomes of the same three accessions of D3 and D4 and three of the four accessions of T2 used for NPQ measurements (excluding G1854 due to unsuccessful Illumina library construction). Illumina RNA-Seq libraries were constructed for each accession (nine) under each of two light treatments, for a total of 18 libraries. High throughput sequencing generated an average of 11.3 million 88 bp reads per library passing quality filtering (minimum library size = 3.5 million, maximum = 23.0 million), of which an average of 24.6%
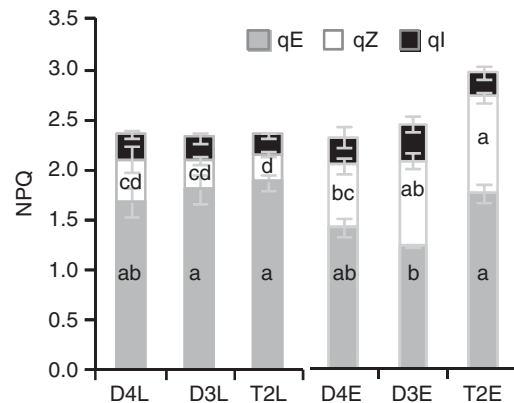

Figure 2 T2 allotetraploids exhibit elevated qE vs D3 diploids and elevated qZ vs D4 diploids under EL. Absolute contributions of qE, qZ and qI to total NPQ capacity (NPQ$_{max}$) under LL (D4L, D3L, T2L) and EL (D4E, D3E, T2E). Error bars represent s.e. ($N = 3$ (D3 and D4) or 4 (T2)). The main effect of light treatment was significant for qE ($F_{1,14} = 39.530$, $P < 0.001$), and qZ ($F_{1,14} = 69.482$, $P < 0.001$), but not qI ($F_{1,14} = 2.171$, $P = 0.163$). The main effect of species was not significant for qE ($F_{2,14} = 3.739$, $P = 0.079$), qZ ($F_{2,14} = 1.076$, $P = 0.368$) or qI ($F_{2,14} = 0.950$, $P = 0.411$). There was a significant interaction between treatment and species for qE ($F_{2,14} = 6.617$, $P = 0.024$) and qZ ($F_{2,14} = 6.553$, $P = 0.010$) but not qI ($F_{2,14} = 0.493$, $P = 0.621$). Letters in columns indicate statistical significance—samples not sharing a letter differ significantly at $P < 0.05$ (Tukey's HSD) for the given NPQ component. No significant differences were observed for qI.
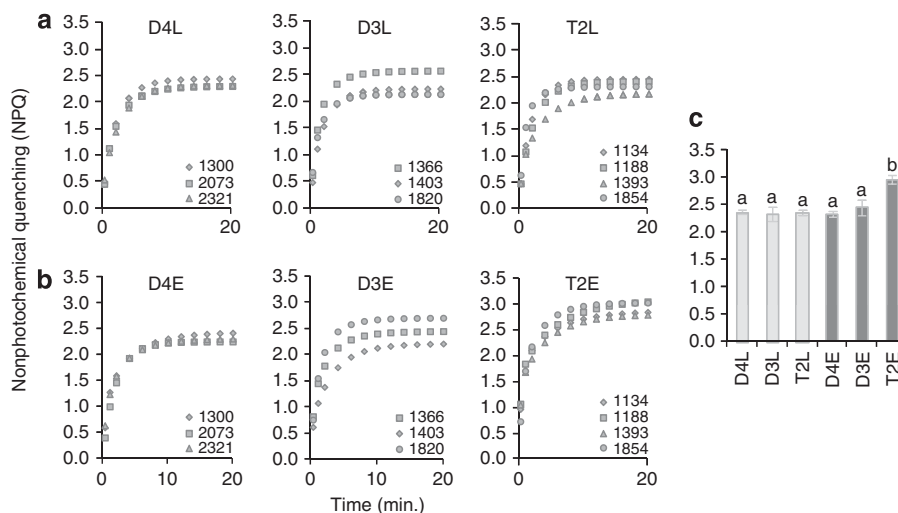

Figure 1 T2 allotetraploids have greater NPQ capacity than their diploid progenitors under EL. Light treatment ($F_{1,14} = 10.378$, $P = 0.006$), species ($F_{2,14} = 8.124$, $P = 0.005$) and their interaction ($F_{2,14} = 7.796$, $P = 0.005$), all had significant effects on NPQ$_{max}$. (**a**) NPQ response curves (NPQ vs time) by accession for plants grown under LL. (**b**) NPQ response curves (NPQ vs time) by accession for plants grown under EL. (**c**) Mean NPQ capacity by species and light treatment. Error bars represent s.e. ($N = 3$ (D3 and D4) or 4 (T2)). Letters above columns indicate statistical significance—categories not sharing a letter differ significantly at $P < 0.05$ (Tukey's HSD).

(20.8–27.5%) were uniquely (unambiguously) mapped to the soybean (*G. max*) reference genome (Schmutz *et al.*, 2010). Uniquely mapped reads were assigned to between 29 364 and 35 419 high confidence protein-coding gene models per library (63.2–76.3% of high confidence protein-coding gene models in the soybean genome; Schmutz *et al.*, 2010). Expression estimates for one gene family (*PsbS*) under both LL and EL were validated by quantitative real-time PCR (data not shown). We have previously validated RNA-Seq-based expression estimates for six additional gene families by quantitative real-time PCR (Coate and Doyle, 2010).

T2 exhibits a smaller overall transcriptional response to EL than D3 or D4. Overall, T2 exhibited a smaller transcriptional response to EL than did either diploid. Changes in expression between EL and LL were generally smaller in T2 than in D3 or D4 (Figure 3), and Pearson correlation coefficients (*r*) of RPKM values were higher between the T2 EL (T2E) and T2 LL (T2L) transcriptomes than between D3E and D3L or D4E and D4L (Supplementary Table S3). T2 also had the fewest genes showing a ⩾twofold change in expression (that is, transcript abundance) between LL and EL, as well as the fewest number of genes identified as significantly differentially expressed between LL and EL (Figure 3, Supplementary Table S4).

Because T2 exhibited enhanced NPQ capacity under EL (Figure 1), we looked to see whether the expression profiles were consistent, with T2 having experienced less photooxidative stress than D3 or D4 under this treatment. Indeed, the diploids exhibited several transcriptional responses associated with photo-oxidative stress that were not observed in T2. Several gene ontology terms related to oxidative stress were over-represented among genes that were significantly upregulated by EL (FDR < 0.05) in one or both diploids but not in T2 (Table 1). By contrast, no gene ontology terms specific to oxidative stress response were over-represented among the genes significantly upregulated by EL in T2 (see Supplementary Table S5 for a full list of over-represented gene ontology categories).

Glutathione peroxidases, which detoxify lipid hydroperoxides (Milla *et al.*, 2003), were upregulated under EL in both D3 (Glyma01g42840 and Glyma 11g02630) and D4 (Glyma01g42840) but not T2. The Arabidopsis protein, salt tolerance zinc finger (STZ; AT1g27730) is a type of zinc-finger protein involved in photo-oxidative stress response (Sakamoto *et al.*, 2004), and five of the six orthologues of the Arabidopsis *STZ* gene were significantly upregulated in response to EL in D3 (Glyma04g04760, Glyma 06g04840, Glyma10g40400, Glyma14g09760 and Glyma20g26940), but none were significantly upregulated in T2. The sum of expression from all *STZ* gene family members (hereafter, 'combined gene family expression') increased fivefold in D3 and 1.8-fold in D4, but remained constant in T2 (onefold). The Arabidopsis *DOX1* gene encodes an α-dioxygenase that is involved in protection against oxidative stress (De León *et al.*, 2002). Combined *DOX1* gene family expression was 3.2-fold higher in D4E than in T2E (FDR = 0.05) and 2.7-fold higher in D3E than in T2E (FDR = 0.16).

Conversely, light harvesting complex (LHC)-encoding genes were more strongly downregulated under EL in D3 and D4 than in T2.

Table 1 Oxidative stress-related gene ontology (GO) terms over-represented among genes upregulated by excess light in D3 and/or D4 but not T2

GO Cat.	GO Term	Description	D3	D4
P	GO:0006950	Response to oxidative stress	Y	Y
P	GO:0034599	Cellular response to oxidative stress	Y	Y
P	GO:0000302	Response to reactive oxygen species	Y	Y
P	GO:0034614	Cellular response to reactive oxygen species	Y	Y
P	GO:0042542	Response to hydrogen peroxide	Y	
P	GO:0070301	Cellular response to hydrogen peroxide		Y
P	GO:0042744	Hydrogen peroxide catabolic process		Y
P	GO:0006800	Reactive oxygen species metabolic process		Y
F	GO:0016209	Antioxidant activity	Y	Y
F	GO:0004601	Peroxidase activity	Y	Y
F	GO:0004364	Glutathione transferase activity	Y	Y
F	GO:0004602	Glutathione peroxidase activity	Y	
P	GO:0009812	Flavonoid metabolic process	Y	Y
P	GO:0009813	Flavonoid biosynthetic process	Y	Y
P	GO:0009699	Phenylpropanoid biosynthetic process	Y	Y
P	GO:0009698	Phenylpropanoid metabolic process	Y	Y

'Y' indicates that the specified GO term is over-represented (false discovery rate < 0.05; Fisher's exact test) among the upregulated genes in that species. GO categories are 'Biological Process' (P) and 'Molecular Function' (F).
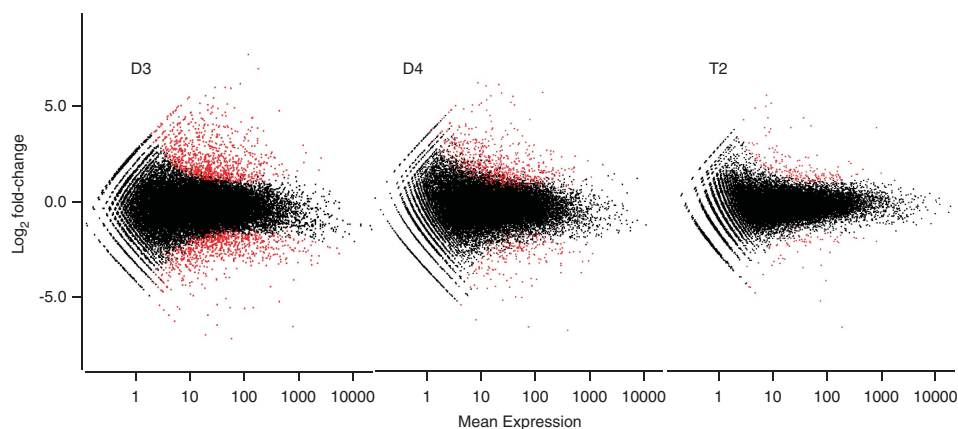

Figure 3 T2 allotetraploids exhibit a smaller transcriptional response to EL than their diploid progenitors. Scatter plots of fold change (log scale) in expression (EL/LL) vs mean expression (average of expression under excess and limting light), as estimated by DESeq. Significant differences (FDR ⩽ 0.05; Benjamini–Hochberg adjustment) are indicated in red, non-significant differences (FDR > 0.05) in black. The smaller transcriptional response to EL in T2 is apparent in both the smaller degree of scatter and fewer significantly differentially expressed genes.

Downregulation of *Lhc* genes is an acclimatory response to EL in which the plant balances light harvesting with the capacity for electron transport (Teramoto *et al.*, 2002), and combined gene family expression was lower in EL than LL in all the three species for 10 out of 14 *Lhc* families (Figure 4). However, in each of these 10 gene families, T2 exhibited a smaller reduction in transcript level than either diploid (Figure 4). Additionally, whereas *LhcA5, LhcA6 and LhcB7* showed subtle downregulation in response to EL in D3 and D4, expression of all the three gene families increased in T2 (1.5–2.4-fold).

Thus, transcriptional profiles indicated that T2 responded less to EL than did D3 or D4 in general and, consistent with enhanced NPQ capacity, showed less activation of genes involved in photo-oxidative stress response. Taken together, this suggests that T2 experienced less stress under EL than did D3 or D4. Next, we examined the expression profiles for clues about the molecular mechanisms underlying the enhanced NPQ phenotype in T2.

Expression patterns suggest upregulation of carotenoid biosynthesis in T2 vs D4 but not D3. Under LL, no genes encoding carotenoid biosynthetic enzymes were upregulated in T2 vs either diploid, and combined gene family expression was comparable among the three species (Supplementary Figures S3A and B). By contrast, three genes encoding phytoene synthase (Glyma02g45270, Glyma08g41890 and

Glyma18g13700), which catalyzes the first step in carotenoid bio-synthesis, were significantly upregulated in T2E vs D4E, and combined gene family expression was 2.5-fold higher in T2E than in D4E (Supplementary Figure S3C). Genes encoding carotene hydroxylase (Glyma16g29790) and phytoene desaturase (Glyma18g00720) were also significantly upregulated in T2E vs D4E, and genes encoding lycopene β-cyclase (Glyma19g31220) and lycopene β/ε-cyclase (Glyma14g05100) were marginally upregulated in T2E vs D4E (FDR = 0.07 for both). Combined gene family expression was > 1.5-fold higher in T2E vs D4E for 11 out of 13 enzymes (Supplementary Figures S3C and D). By comparison, differences in EL expression between T2 and D3 for these carotenoid biosynthetic genes were uniformly smaller (Supplementary Figures S3C and D). Thus, expression of genes encoding enzymes of carotenoid biosynthesis and the xanthophyll cycle generally mirror the qZ phenotype under EL, which was significantly higher in T2 than in D4 but comparable between T2 and D3 (Figure 2).

Expression patterns suggest upregulation of non-photosynthetic electron flows in T2. Two genes upregulated in T2E vs D3E encode copper/zinc superoxide dismutases (CuZn-SOD; Glyma12g08650 and Glyma12g30260) and seven encode peroxidase superfamily proteins (Table 2). CuZn-SOD and ascorbate peroxidase function in the water–water cycle, which represents an alternative pathway to photosynthesis for electron flow, thereby functioning as a safety valve to dissipate energy under EL stress (Asada, 1999). Additionally, by facilitating electron flow from PSII to PSI, the water–water cycle contributes to the formation of a trans-thylakoid pH gradient required for optimal NPQ (Muller-Moule *et al.*, 2002).

In addition to the two *CuZn-SOD* genes identified above, a third *CuZn-SOD* (Glyma11g19840) also showed upregulation in T2E vs both T2L (2.1-fold) and D3E (2.0-fold), though these differences were not statistically significant (Supplementary Figure S4). All the three genes were also upregulated in T2E vs D4E (2.6–5.5-fold) though the differences were only significant for two of these (Glyma11g19840 and Glyma12g08650). All three proteins were predicted to be chloroplast-localized by Predotar (http://urgi.versailles.inra.fr/predotar/predotar.html) and TargetP (http://www.cbs.dtu.dk/services/TargetP/). Four additional genes in the soybean genome are annotated as *CuZn-SODs* but three lack identifiable targeting signals, and Predotar and TargetP gave contradictory predictions for the fourth. None of these four additional *CuZn-SODs* were significantly upregulated in T2E vs T2L, D3E or D4E. Thus, T2 specifically upregulated plastid-localized *CuZn-SODs* in response to EL and in comparison to its diploid progenitors.

Several genes involved in CEF-PSI were upregulated in T2E relative to D4E (Table 2).CEF-PSI, like the water–water cycle, represents an alternative pathway for electron flow in the thylakoid electron transport chain that likely has an important role in triggering and maintaining NPQ (Joliot and Johnson, 2011). CEF-PSI involves the shuttling of electrons between PSI and the cytochrome b_6/f complex (Cyt b_6/f) and includes two partially redundant pathways—the NAD(P)H dehydrogenase (NDH) pathway requiring the NDH complex and the proton gradient regulation 5 (PGR5) pathway that functions independently of NDH and requires the proteins PGR5 and proton gradient regulation like 1 (PGRL1; Munekage *et al.*, 2004; Ifuku *et al.*, 2011; Johnson, 2011).

Of the 20 nuclear-encoded subunits of the NDH complex identified by Ifuku *et al.* (2011), genes encoding 11 were upregulated in T2E vs D4E (Table 2). These included genes encoding LHCA5 and LHCA6, which are required for the formation of an NDH-PSI supercomplex that stabilizes NDH, particularly under EL (Ifuku *et al.*, 2011).
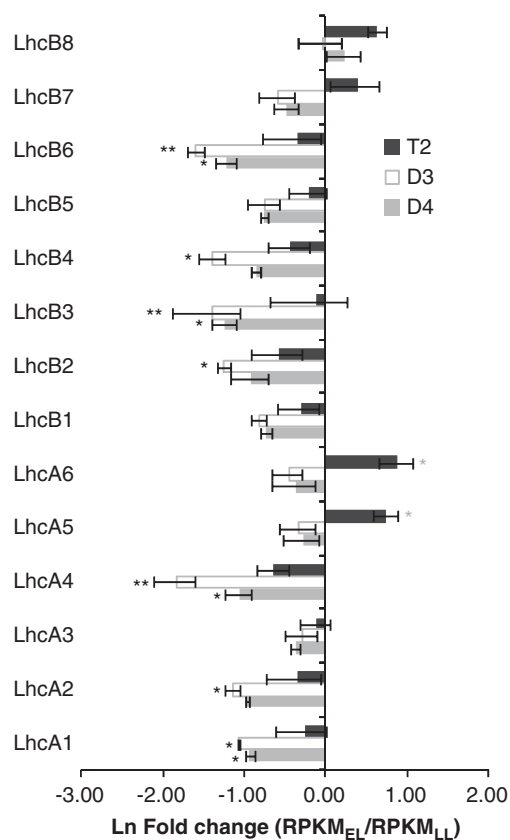

Figure 4 T2 allotetraploids exhibit less downregulation of LHC gene families than their diploid progenitors in response to EL. Fold change in combined gene family expression (the sum of expression from all gene family members) from limiting to EL for each of the 12 LHC gene families (LhcA1-6 and LhcB1-6). Error bars represent s.e. ($N = 3$). Expression data were derived from RNA-Seq transcript profiles. Single asterisks indicate differences in expression between EL and LL with an unadjusted *p*-value < 0.05. Double asterisks indicate differences in expression with FDR < 0.05 (Benjamini–Hochberg adjustment). Significance levels were determined using DESeq.

Table 2 Genes upregulated in T2 vs D3 and/or D4 under excess light that are involved in the water–water cycle and/or cyclic electron flow around photosystem I

Pathway/ complex	Annotation	Gene	T2E vs D3E	T2E vs D4E	D3E vs D4E	T2E vs T2L	D3E vs D3L	D4E vs D4L
Water–water	CuZn-SOD	Glyma12g08650	++	++		++	−	−−
		Glyma12g30260	++	+		++	−−	−
		Glyma11g19840	+	++		+	−	
	Peroxidase/APX	Glyma15g41280	++	++				
		Glyma13g20170	++	−−	−−	++		++
		Glyma14g05850	++		−−			
		Glyma01g36780	++		−	+		
		Glyma20g30910	++		−−			++
		Glyma13g04410	++		−−			
		Glyma17g20450	++					
		Glyma13g23620		++	++		+	
		Glyma14g35440		++			−−	
		Glyma02g37160		++			−−	−−
CEF-PSI	NDF1	Glyma08g23400		++	++	++		
		Glyma07g02610		++	++	++		
	NDF4	Glyma13g43260	++	++		++		
		Glyma15g02080		++	+	+		−
	NDF6	Glyma06g20990		++	+	+		
	NDHN	Glyma18g05640		++				
	CRR3	Glyma07g23800		++		++		
	CRR21	Glyma06g23620		++			−	−
	CRR23	Glyma05g27080		++				
	CRR31	Glyma03g01720		++	+			
	PPL2	Glyma20g38370		++	+	+		
		Glyma20g23100		++	++	+		
	FKB16–2	Glyma08g14740		++	+			−
	NQR	Glyma04g27580	++		−−			++
	LhcA5	Glyma04g04110		++		+		
	LhcA6	Glyma09g08260		++			−	
		Glyma15g19810		++		+		
	STN8	Glyma18g44800	++	++		+	−	
		Glyma16g34620		++				
	Fd	Glyma12g29110		++	+			−
		Glyma08g20110		++			−	−
PS I	PsaH	Glyma13g43370		++			−−	−−
	PsaN	Glyma04g39370		++	+		−−	−
	PsaO	Glyma12g09730	++	++		−	−−	−−
	PSI-P	Glyma16g02010	++		−		−	
		Glyma03g42240		++				
		Glyma19g44990		++	+			
Cyt b$_6$f	PetE/cupredoxin	Glyma06g10500	++				−	−
		Glyma14g35530	++					
		Glyma19g25570	++		−		−−	
		Glyma02g37210	++		−		−	
		Glyma04g02240		++	+		−	
	PetM	Glyma06g03920	++				−	−
	HCF107	Glyma07g36870	++		−		−	−

Abbreviations: APX, ascorbate peroxidase; CEF-PSI, cyclic electron flow around photosystem I; Fd, ferredoxin.
For each column, genes that are overexpressed in the first sample vs the second sample are indicated by '+' (unadjusted p-value <0.05) or '++' (false discovery rate (FDR)<0.05); genes that are underexpressed in the first sample vs the second sample are indicated by '−' (unadjusted p-value <0.05) or '−−' (FDR<0.05).

Notably, the expression levels of *LhcA5* and *LhcA6* increased in response to EL in T2 but decreased in both D3 and D4 (Figure 4).

An additional gene upregulated in T2E vs D4E, Glyma06g26320, encodes chlororespiratory reduction 21 (CRR21), which is a pentatricopeptide repeat protein involved in RNA editing of the chloroplast-encoded NDH subunit, NDHD (Okuda *et al.*, 2007). This suggests that plastid genes encoding NDH subunits were upregulated in T2E vs D4E as well.

Of the remaining NDH subunits for which we did not detect significant expression differences, combined gene family expression was nonetheless 1.5–2.5-fold higher in T2E than in D4E. Similarly, though we did not detect significant expression differences in *Pgr5* or

Pgrl1, genes required for the PGR5 pathway, the combined gene family expression was 2.2- and 3.0-fold higher, respectively, in T2E than in D4E. Additionally, the thylakoid-bound kinase, STN8, which phosphorylates PGRL1 and has a critical role in regulating the PGR5 pathway (Reiland *et al.*, 2011), was significantly upregulated in T2E vs D4E (Table 2).

Both CEF-PSI pathways require PSI, Cyt b$_6$/f, ferredoxin and ferredoxin-NADP reductase (FNR; Joliot and Johnson, 2011; Johnson, 2011). Compared with D4E, T2E also over-expressed genes encoding several PSI subunits (PsaH, PsaN, PsaO and PSI-P), the Cyt b$_6$F subunit, plastocyanin and ferredoxin (Table 2). Additionally, though the differences were not significant at FDR = 0.05, combined gene family expression was 2.1-fold higher for the Cytb$_6$f subunit *PetM* and 1.8-fold higher for the leaf-type *FNR* in T2E relative to D4E. We observed notably fewer differences in expression relating to CEF-PSI between T2E and D3E (Table 2).

Combined gene family expression for most PSI and Cyt b$_6$f subunits was higher in T2E than in either diploid, though the differences were consistently smaller between T2E and D3E than between T2E and D4E (Supplementary Figure S5). PSI has a central role in both the water–water cycle and CEF-PSI. This suggests that T2 has enhanced water–water cycle capacity relative to both diploid progenitors (via upregulation of CuZn-SOD, *Cyt b6f* and PSI), as well as enhanced CEF-PSI relative to D4, but not D3, via upregulation of CEF-PSI genes.

Quantum yield of photosystem II (Φ_{PSII})

Enhanced Φ_{PSII} in T2 is consistent with upregulation of non-photosynthetic electron flows under EL. We measured NPQ in the absence of CO_2. Electron transport observed under these conditions would be facilitated by non-photosynthetic pathways, including the water–water cycle. If T2 had a higher capacity for this pathway, as suggested by the transcript profiling data, we would expect to see differences between T2 and its diploid progenitors in the quantum yield of PSII (Φ_{PSII}) under these measurement conditions. When grown under LL, Φ_{PSII} was comparable among the three species, and T2 exhibited the slowest rate of Φ_{PSII} increase during the first minute of illumination, though the differences were not significant (Figures 5a and c). There was a significant effect of light treatment on Φ_{PSII} ($F_{1,14} = 287.513$, $P < 0.001$), with all the three species exhibiting increases in steady state Φ_{PSII} under EL (Figure 5c), indicating that alternative electron transport pathways (other than linear electron flow driving CO_2 fixation) were upregulated in all the three. In contrast to having the slowest initial rise in Φ_{PSII} upon illumination under LL, T2 exhibited the fastest initial rise under EL, as well as the highest steady state Φ_{PSII}, though neither difference was statistically significant under the general linear model (Figures 5b and c). A single-factor analysis of variance did detect a significant effect of species under EL ($F_{2,7} = 5.229$, $P = 0.041$), with T2 significantly higher than D4 ($P = 0.035$; Tukey's HSD).

DISCUSSION

Polyploidy has been shown to increase photosynthetic capacity per cell in many taxa (citations in Warner and Edwards, 1993), and we have shown that this is true in the recently formed natural allotetraploid, *G. dolichocarpa* (T2) (Coate *et al.*, 2012; Ilut *et al.*, 2012). Here we showed that under conditions of chronic EL, NPQ capacity (NPQ$_{max}$) is also significantly enhanced in T2 relative to its diploid progenitors. Because T2 has a greater capacity for both photochemical and NPQ, the observed increase in NPQ$_{max}$ is not simply a mechanism to compensate for lower photochemical capacity.
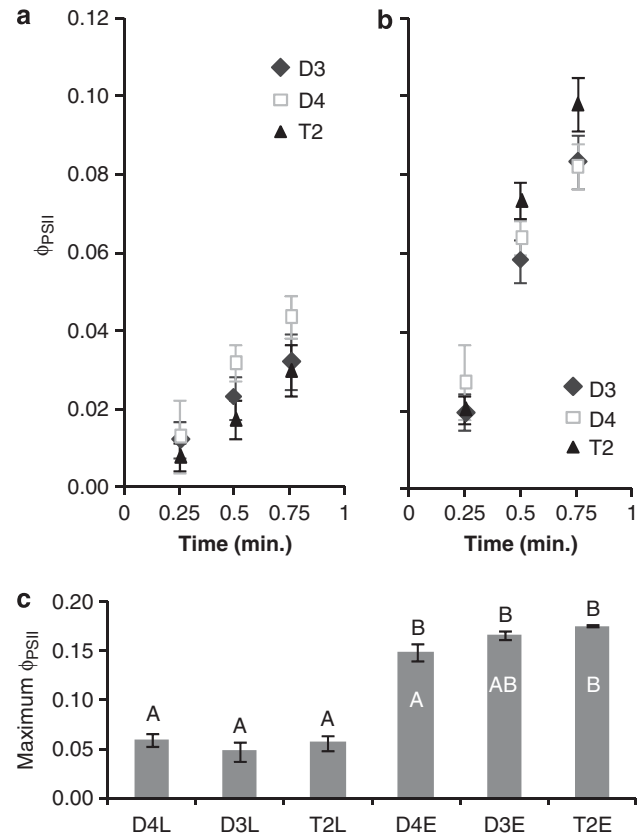

Figure 5 Excess light-acclimated T2 exhibits a faster rise in quantum yield of photosystem II (Φ_{PSII}), and/or higher maximum Φ_{PSII}, than its diploid progenitors under NPQ measurement conditions (2000 µmol m^{-2} s^{-1} light intensity, 0% CO_2, 2% O_2). Under the general linear model (GLM), the main effect of light treatment had a significant effect on Φ_{PSII} ($F_{1,14} = 287.513$, $P < 0.001$), but species ($F_{2,14} = 1.055$, $P = 0.374$), and the interaction of treatment and species ($F_{2,14} = 2.629$, $P = 0.107$) were not significant. A single-factor analysis of variance testing the effect of species on Φ_{PSII} under EL did detect a significant effect ($F_{2,7} = 5.229$, $P = 0.041$). (**a**) Initial rise in Φ_{PSII} during the first minute of illumination for plants grown under LL. (**b**) Initial rise in Φ_{PSII} during the first minute of illumination for plants grown under EL. (**c**) Maximum Φ_{PSII} achieved during NPQ measurement for plants grown under LL (D4L, D3L, T2L) and EL (D4E, D3E, T2E). Letters above columns indicate statistical significance between samples under the GLM—categories not sharing a letter differ significantly at $P < 0.05$ (Tukey's HSD). White letters inside the EL columns indicate statistical significance between species within EL based on a single-factor analysis of variance comparing differences among species under EL (Tukey's HSD). In all the three panels, error bars represent s.e. ($N = 3$ (D3 and D4) or 4 (T2)).

Additionally, when grown under light conditions that are limiting to photosynthesis (LL), and therefore unlikely to result in significant EL stress, the polyploid exhibited NPQ capacity comparable to its diploid progenitors. Therefore, the observed increase in NPQ$_{max}$ may represent a capacity to acclimate to EL rather than a constitutively activated trait that might be maladaptive under limiting or variable light conditions (Kulheim *et al.*, 2002; Krah and Logan, 2010).

NPQ represents thermal dissipation of excess energy, which serves to prevent photooxidative damage. Though we did not detect significant differences in photoinhibitory quenching (qI), this component was smallest in T2. Consequently, the enhanced capacity for NPQ in T2 may have resulted in less damage to PSII reaction centers.

Additionally, our transcript profiling data suggest that T2 mounts less of a photoxidative stress response under EL than do D3 or D4. This further supports the conclusion that the enhanced capacity for T2 to increase NPQ under chronic EL is advantageous. By doing so, T2 appears to experience less photo-oxidative stress and does not need to activate defenses against photo-oxidative damage to the same extent as its diploid progenitors. In further support of this conclusion, though all plants began to show visible signs of photo-oxidative stress (for example, photobleaching) after several weeks under EL, these signs were generally slower to develop and less severe in T2 than in D3 or D4 (data not shown).

As with NPQ_{max}, no differences among the three species were observed in any of the three individual components of NPQ (qE, qZ or qI) under LL. In both LL and EL, qE was the largest component, and qI the smallest component, of NPQ in all the three species. Similarly, all the three exhibited the same qualitative responses to EL (decreased qE and increased qZ and qI). It appears that T2 achieved a transgressive NPQ phenotype (greater NPQ_{max}) by combining the best aspects of its diploid progenitors. Specifically, T2 maintained a level of qE comparable with D4 but greater than D3 and a level of qZ comparable with D3 but greater than D4.

The fact that qE decreased under EL in all the three species is not surprising as qE is a rapidly reversible form of NPQ that is thought to be of greatest importance in dealing with rapidly fluctuating light conditions (Kulheim et al., 2002; Krah and Logan, 2010). Under the chronic EL conditions in which these plants were grown, it would make sense that the overall strategy for energy dissipation would shift to a more sustained mechanism. Zeaxanthin-dependent quenching (qZ) is a more slowly relaxing form of NPQ than qE, yet is still reversible (that is, does not represent damage to the PSII reaction center; Melkonnian et al., 2004; Nilkens et al., 2010). In all three species, qZ was greater in plants grown under EL than in plants grown under LL.

Both qE and qZ require formation of a pH gradient (ΔpH) across the thylakoid membrane (Munekage et al., 2004). Under our measurement conditions wherein carbon fixation is limiting to electron flow, both the water–water cycle (Neubauer and Yamamoto, 1992; Rizhsky et al., 2003; Murchie and Niyogi, 2011) and CEF-PSI (Miyake et al., 2004; Munekage et al., 2004; Johnson, 2011) are thought to have important roles in the formation of this gradient.

In the water–water cycle, electrons derived from water at PSII are transferred via the Cyt b_6f complex to PSI and then to O_2, generating superoxide (O_2^-). O_2^- is dismuted to O_2 and H_2O_2 by chloroplast-localized CuZn-SOD, and H_2O_2 is reduced to water by ascorbate peroxidase (Neubauer and Yamamoto, 1992). Thus, electrons are transported from PSII to PSI with no net oxygen evolution, generating a ΔpH across the thylakoid membrane.

Under EL, T2 upregulated chloroplast-localized CuZn-SOD genes, as well as several peroxidases, including genes annotated as ascorbate peroxidases, relative to both D3 and D4. Thus, the expression data suggest that T2 may upregulate the water–water cycle relative to either diploid progenitor in response to EL. This is supported by the fact that T2E exhibits a numerically (though not statistically significantly) faster initial rise in the quantum yield of PSII (Φ_{PSII}) than D3E or D4E, and significantly higher steady state Φ_{PSII} compared with D4E (but not D3E), in the absence of CO_2 (Figure 5). In turn, this could facilitate rapid formation of a trans-thylakoid pH gradient necessary for qE (Muller-Moule et al., 2002). Because T2 overexpresses water–water cycle genes relative to both D3 and D4, enhanced water–water cycle capacity could explain the enhanced qE phenotype in T2,

which was significantly higher than in D3, and numerically but not statistically significantly higher than in D4 ($P = 0.097$; Supplementary Table S2; Figure 2). In this context, it is notable that the water–water cycle is particularly active during the transition from darkness to light (Murchie and Niyogi, 2011) and therefore likely has a key role in establishing the ΔpH necessary for qE (Asada, 1999; Murchie and Niyogi, 2011).

CEF-PSI, which involves the cycling of electrons between PSI and the Cyt b_6f complex (Johnson, 2011), also produces a ΔpH across the thylakoid membrane, is activated when photosynthetic linear electron flow is saturated (Miyake et al., 2004) and has an important role in NPQ (Joliot and Johnson, 2011). CEF-PSI is mediated by two partially redundant pathways—the NDH pathway and the PGR5 pathway (Munekage et al., 2004; Ifuku et al., 2011; Johnson, 2011). Mutants of Arabidopsis defective in the PGR5 pathway are impaired in their ability to form a ΔpH under EL and exhibit slower induction of NPQ and impaired NPQ capacity in CO_2-free air or EL (Munekage et al., 2002; 2004). By contrast, Arabidopsis mutants defective in the NDH pathway do not exhibit impaired ΔpH or NPQ (Munekage et al., 2004), but NDH genes are upregulated in response to photo-oxidative stress in tobacco (Wang et al., 2006), and tobacco NDH mutants exhibit increased photoinhibition and chlorosis under saturating light compared with wildtype (Endo et al., 1999). Thus, it is generally accepted that the NDH pathway functions in photo-protection, if not directly in ΔpH-dependent NPQ (Wang et al., 2006; Ifuku et al., 2011).

Our expression data suggest that both CEF-PSI pathways are upregulated in T2 relative to D4 under EL. By contrast, T2 exhibited few differences in expression relative to D3 for genes involved in CEF-PSI. Thus, it is possible that T2 has a capacity for CEF-PSI that is greater than that of D4 but comparable with D3. We observed similar expression patterns for genes of the carotenoid biosynthetic pathway and xanthophyll cycle. Genes encoding most of these enzymes were upregulated in T2E vs D4E but comparable between T2E and D3E.

qZ requires the conversion of violaxanthin to zeaxanthin by the xanthophyll cycle enzyme, VDE. VDE is activated by the thylakoid ΔpH, which is generated by CEF-PSI under saturating light. Consequently, we speculate that under chronic EL T2 generates a larger xanthophyll pool, more VDE and a greater capacity for CEF-PSI than D4, which together explain the enhanced qZ phenotype in T2 vs D4. Conversely, the expression data suggest that T2 and D3 have comparable amounts of xanthophylls and VDE and equivalent CEF-PSI capacities under EL, which is consistent with the fact that qZ capacity is also comparable between the two.

It should of course be emphasized that our conclusions regarding the water–water cycle, CEF-PSI and the xanthophyll cycle are based upon transcript profiles and are only valid if fluxes through these pathways correlate with transcript abundance. It should also be noted that the extent of upregulation in T2E vs D3E or D4E of genes involved in these processes may in fact be underestimated. We have demonstrated previously that the T2L transcriptome is 1.4-fold larger than both the D3L and D4L transcriptomes (Coate and Doyle, 2010). We have not quantified EL transcriptome size for these species but have shown that a related allopolyploid (T5) also has a ca. 1.5-fold larger LL leaf transcriptome than its diploid progenitors (unpublished data). This suggests that larger transcriptome size is a general property of Glycine allopolyploids. Based on this observation, and the fact that T2 has at least 1.87 times as many genes as its diploid progenitors (Coate and Doyle, 2010), it seems likely that the T2E transcriptome is also larger than the D3E or D4E transcriptomes. RNA-Seq gene expression estimates are transcriptome normalized

(transcript abundance for an individual gene is given relative to total transcript abundance, that is, RPKM; Coate and Doyle, 2010). Therefore, if the T2E transcriptome is larger than the transcriptomes of its diploid progenitors, RPKM will underestimate differences in expression per cell for genes that are upregulated. Therefore, we consider it likely that the extent of upregulation in gene networks involved in the water–water cycle, CEF-PSI and carotenoid biosynthesis are in fact higher than reported here.

Overall, therefore, we suggest that in order to manage chronic EL, T2 is able to upregulate the water–water cycle relative to both diploid progenitors, as well as carotenoid biosynthesis, the xanthophyll cycle and CEF-PSI relative to D4. This results in a greater capacity for thermal dissipation of excess energy (NPQ) and may result in less photooxidative stress.

General significance

Polyploids frequently exhibit broader geographic ranges and occupy more extreme habitats than their diploid progenitors, prompting speculation that polyploids have a greater ability to tolerate stress (Otto and Whitton, 2000; Ramsey, 2011). Our data provide a concrete example of how one polyploid species may be better equipped to tolerate a particular abiotic stress than its diploid progenitors.

It is possible that the enhanced NPQ phenotype in T2 is the result of adaptation to habitats with higher light intensities and that such adaptation is unrelated to allopolyploidy. However, the D3, D4 and T2 species ranges overlap in Queensland, Australia, with all frequently growing in open habitats (for example, open woodland or grassland), and T2 is found in shaded habitats more frequently than are D3 or D4 (Brown ADH, personal communication). Thus, it is likely that T2, D3 and D4 have experienced similar selective pressures on NPQ capacity, suggesting that intrinsic factors, such as hybridity and/or ploidy level, may have contributed to the observed differences.

It is tempting to speculate that enhanced NPQ had a role in both the origin of T2 as well as the expansion of its geographical range relative to those of its progenitors. T2, as well as seven other allopolyploid species in Glycine subgenus Glyine, originated in Australia within the past 50 000 to 100 000 years (Doyle et al., 2004), a timeframe corresponding to major environmental changes (Hope, 1994). The last ice age began approximately 60 000 years ago, resulting in significant cooling and drying. At approximately the same time, humans first colonized the continent and altered the vegetation by burning (Hudjashov et al., 2007; Notaro et al., 2011). Combined, these events presumably opened new niches characterized by increased exposure to direct sunlight and decreased moisture and temperature—conditions likely to induce photoinhibition and place a premium on photoprotective mechanisms. Because polyploidy is a common phenomenon in plants, it is likely that allopolyploids have been produced throughout the history of Glycine subgenus Glycine. We speculate that allopolyploids became established in the subgenus during this time—as at no previous time in its history—in part because allopolyploidization resulted in enhanced photoprotective capabilities. This hypothesis could be more explicitly tested with common garden experiments in which T2, D3 and D4 are grown together under limiting and EL conditions, with the expectation that T2 would exhibit an improvement in fitness (for example, seed yields) relative to its diploid progenitors under EL compared with LL.

In addition, all of the diploid species in Glycine subgenus Glycine are confined to Australia or the eastern tip of Papua New Guinea. By contrast, five of the eight allopolyploid species in the subgenus have colonized islands of the Pacific Ocean as far north as Japan (Doyle et al., 2004). T2 has colonized Taiwan (Doyle et al., 2004),

ca. 5000 km from its putative origins in Australia (Doyle et al., 2002), thereby dramatically expanding its geographic range beyond that of its diploid progenitors. In Taiwan, T2 is typically found in open habitats characterized by high light intensities. Perhaps an enhanced capacity to manage EL stress contributed to the ability of Glycine subgenus Glycine allopolyploids to colonize new habitats.

Anders S, Huber W (2010). Differential expression analysis for sequence count data. Genome Biol 11: R106.
Asada K (1999). The water–water cycle in chroroplasts: scavenging of active oxygens and dissipation of excess photons. Annu Rev Plant Physiol Plant Mol Biol 50: 601–639.
Avenson TJ, Cruz JA, Kramer DM (2004). Modulation of energy-dependent quenching of excitons in antennae of higher plants. Proc Natl Acad Sci USA 101: 5530–5535.
Baker NR (2008). Chlorophyll fluorescence: a probe of photosynthesis in vivo. Annu Rev Plant Biol 59: 89–113.
Coate JE, Doyle JJ (2010). Quantifying whole transcriptome size, a prerequisite for understanding transcriptome evolution across species: an example from a plant allopolyploid. Genome Biol Evol 2: 534–546.
Coate JE, Luciano AK, Seralathan V, Minchew KJ, Owens TG, Doyle JJ (2012). Anatomical, biochemical, and photosynthetic responses to recent allopolyploidy in Glycine dolichocarpa (Fabaceae). Am J Bot 99: 55–67.
De León IP, Sanz A, Hamberg M, Castresana C (2002). Involvement of the Arabidopsis?-DOX1 fatty acid dioxygenase in protection against oxidative stress and cell death. Plant J 29: 61–72.
Demmig-Adams B, Adams WW, Heber U, Neimanis S, Winter K, Kruger A et al. (1990). Inhibition of zeaxanthin formation and of rapid changes in radiationless energy dissipation by dithiothreitol in spinach leaves and chloroplasts. Plant Physiol 92: 293–301.
Demmig-Adams B, Ebbert V, Mellman DL, Mueh KE, Schaffer L, Funk C et al. (2006). Modulation of PsbS and flexible vs sustained energy dissipation by light environment in different species. Physiol Plantarum 127: 670–680.
Demmig-Adams B, Adams WW (2000). Photosynthesis: harvesting sunlight safely. Nature 403: 371–374.
Doyle JJ, Doyle JL, Brown AHD, Palmer RG (2002). Genomes, multiple origins, and lineage recombination in the Glycine tomentella (Leguminosae) polyploid complex: histone H3-D gene sequences. Evolution 56: 1388–1402.
Doyle JJ, Doyle JL, Rauscher JT, Brown AHD (2004). Evolution of the perennial soybean polyploid complex (Glycine subgenus Glycine): a study of contrasts. Biol J Linn Soc 82: 583–597.
Dunstone R, Evans L (1974). Role of changes in cell size in the evolution of wheat. Funct Plant Biol 1: 157–165.
Ehrendorfer F (1980). Polyploidy and distribution. In Polyploidy: Biological Relevance. (ed Lewis WH) Plenum: NY, pp 45–60.
Endo T, Shikanai T, Takabayashi A, Asada K, Sato F (1999). The role of chloroplastic NAD(P)H dehydrogenase in photoprotection. FEBS Lett 457: 5–8.
Hope GS (1994). Quaternary vegetation. In History of the Australian Vegetation: Cretaceous to RecentHill RS (eds). Cambridge University Press: New York, NY, pp 368–389.
Horton P, Ruban A (2005). Molecular design of the photosystem II light-harvesting antenna: photosynthesis and photoprotection. J Exp Bot 56: 365–373.
Horton P, Johnson MP, Perez-Bueno ML, Kiss AZ, Ruban AV (2008). Photosynthetic acclimation: does the dynamic structure and macro-organisation of photosystem II in higher plant grana membranes regulate light harvesting states? Febs J 275: 1069–1079.
Hudjashov G, Kivisild T, Underhill PA, Endicott P, Sanchez JJ, Lin AA et al. (2007). Revealing the prehistoric settlement of Australia by Y chromosome and mtDNA analysis. Proc Natl Acad Sci USA 104: 8726–8730.

Ifuku K, Endo T, Shikanai T, Aro E (2011). Structure of the chloroplast NADH dehydrogenase-like complex: nomenclature for nuclear-encoded subunits. *Plant Cell Physiol* **52**: 1560–1568.

Ilut DC, Coate JE, Luciano AK, Owens TG, May GD, Farmer AD et al. (2012). A comparative transcriptomic study of an allotetraploid and its diploid progenitors illustrates the unique advantages and challenges of RNA-Seq in plant species. *Am J Bot* **99**: 383–396.

Innes RW, Ameline-Torregrosa C, Ashfield T, Cannon E, Cannon SB, Chacko B et al. (2008). Differential accumulation of retroelements and diversification of NB-LRR disease resistance genes in duplicated regions following polyploidy in the ancestor of soybean. *Plant Physiol* **148**: 1740–1759.

Jiao Y, Wickett NJ, Ayyampalayam S, Chanderbali AS, Landherr L, Ralph PE et al. (2011). Ancestral polyploidy in seed plants and angiosperms. *Nature* **473**: 97–100.

Johnson GN, Young AJ, Scholes JD, Horton P (1993). The dissipation of excess excitation energy in British plant species. *Plant Cell Environ* **16**: 673–679.

Johnson GN (2011). Reprint of: Physiology of PSI cyclic electron transport in higher plants. *Biochim Biophys Acta* **1807**: 906–911.

Joliot P, Joliot A (2002). Cyclic electron transfer in plant leaf. *Proc Natl Acad Sci USA* **99**: 10209–10214.

Joliot P, Johnson GN (2011). Regulation of cyclic and linear electron flow in higher plants. *Proc Natl Acad Sci USA* **108**: 13317–13322.

Krah NM, Logan BA (2010). Loss of *psbS* expression reduces vegetative growth, reproductive output, and light limited, but not light saturated, photosynthesis in *Arabidopsis thaliana* (Brassicaceae) grown in temperate environments. *Am J Bot* **97**: 644–649.

Krause GH, Jahns P (2004). *Non-photochemical energy dissipation determined by chlorophyll fluorescence quenching: characterization and function. In Chlorophyll a Fluorescence: A Signature of Photosynthesis.* (eds Papageorgiou GC, Govindjee) Springer: Dordrecht, The Netherlands, pp 463–495.

Kulheim C, Agren J, Jansson S (2002). Rapid regulation of light harvesting and plant fitness in the field. *Science* **297**: 91–93.

Lambrev PH, Nilkens M, Miloslavina Y, Jahns P, Holzwarth AR (2010). Kinetic and spectral resolution of multiple nonphotochemical quenching components in Arabidopsis leaves. *Plant Physiol* **152**: 1611–1624.

Lewis WH (1980). *Polyploidy in species populations. In Polyploidy: Biological Relevance.* Lewis WH (eds). Plenum: NY, pp 103–144.

Li XP, Bjorkman O, Shih C, Grossman AR, Rosenquist M, Jansson S et al. (2000). A pigment-binding protein essential for regulation of photosynthetic light harvesting. *Nature* **403**: 391–395.

Li XP, Muller-Moule P, Gilmore AM, Niyogi KK (2002). PsbS-dependent enhancement of feedback de-excitation protects photosystem II from photoinhibition. *Proc Natl Acad Sci USA* **99**: 15222–15227.

Li Z, Wakao S, Fischer BB, Niyogi KK (2009). Sensing and responding to excess light. *Annu Rev Plant Biol* **60**: 239–260.

Maxwell K, Johnson GN (2000). Chlorophyll fluorescence - a practical guide. *J Exp Bot* **51**: 659–668.

Melkonian J, Owens TG, Wolfe DW (2004). Gas exchange and co-regulation of photochemical and nonphotochemical quenching in bean during chilling at ambient and elevated carbon dioxide. *Photosynthesis Res* **79**: 71–82.

Milla MAR, Maurer A, Huete AR, Gustafson JP (2003). Glutathione peroxidase genes in Arabidopsis are ubiquitous and regulated by abiotic stresses through diverse signaling pathways. *Plant J* **36**: 602–615.

Miyake C, Shinzaki Y, Miyata M, Tomizawa K (2004). Enhancement of cyclic electron flow around PSI at high light and its contribution to the induction of non-photochemical quenching of Chl fluorescence in intact leaves of tobacco plants. *Plant Cell Physiol* **45**: 1426–1433.

Molin WT, Meyers SP, Baer GR, Schrader LE (1982). Ploidy effects in isogenic populations of alfalfa: II. Photosynthesis, chloroplast number, ribulose-1,5-bisphosphate carboxylase, chlorophyll, and DNA in protoplasts. *Plant Physiol.* **70**: 1710–1714.

Mortazavi A, Williams BA, McCue K, Schaeffer L, Wold B (2008). Mapping and quantifying mammalian transcriptomes by RNA-Seq. *Nat Meth* **5**: 621–628.

Müller-Moulé P, Conklin PL, Niyogi KK (2002). Ascorbate deficiency can limit violaxanthin de-epoxidase activity in vivo. *Plant Physiol* **128**: 970–977.

Munekage Y, Hojo M, Meurer J, Endo T, Tasaka M, Shikanai T (2002). PGR5 is involved in cyclic electron flow around photosystem I and is essential for photoprotection in Arabidopsis. *Cell* **110**: 361–371.

Munekage Y, Hashimoto M, Miyake C, Tomizawa K, Endo T, Tasaka M et al. (2004). Cyclic electron flow around photosystem I is essential for photosynthesis. *Nature* **429**: 579–582.

Murchie EH, Niyogi KK (2011). Manipulation of photoprotection to improve plant photosynthesis. *Plant Physiol* **155**: 86–92.

Neubauer C, Yamamoto HY (1992). Mehler-peroxidase reaction mediates zeaxanthin formation and zeaxanthin-related fluorescence quenching in intact chloroplasts. *Plant Physiol* **99**: 1354–1361.

Nilkens M, Kress E, Lambrev P, Miloslavina Y, Müller M, Holzwarth AR et al. (2010). Identification of a slowly inducible zeaxanthin-dependent component of non-photochemical quenching of chlorophyll fluorescence generated under steady-state conditions in Arabidopsis. *Biochim Biophys Acta* **1797**: 466–475.

Niyogi KK (2000). Safety valves for photosynthesis. *Curr Opin Plant Biol* **3**: 455–460.

Niyogi KK, Li XP, Rosenberg V, Jung HS (2005). Is PsbS the site of non-photochemical quenching in photosynthesis? *J Exp Bot* **56**: 375–382.

Notaro M, Wyrwoll K, Chen G (2011). Did aboriginal vegetation burning impact on the Australian summer monsoon? *Geophys Res Lett* **38**: L11704.

Okuda K, Myouga F, Motohashi R, Shinozaki K, Shikanai T (2007). Conserved domain structure of pentatricopeptide repeat proteins involved in chloroplast RNA editing. *Proc Natl Acad Sci USA* **104**: 8178–8183.

Otto SP, Whitton J (2000). Polyploid incidence and evolution. *Annu Rev Genet* **34**: 401–437.

Pfeil BE, Craven LA, Brown AHD, Murray BG, Doyle JJ (2006). Three new species of northern Australian *Glycine* (Fabaceae, Phaseolae), *G. gracei*, *G. montis-douglas* and *G. syndetika*. *Aust Syst Bot* **19**: 245–258.

Ramsey J (2011). Polyploidy and ecological adaptation in wild yarrow. *Proc Natl Acad Sci USA* **108**: 7096–7101.

Reiland S, Finazzi G, Endler A, Willig A, Baerenfaller K, Grossmann J et al. (2011). Comparative phosphoproteome profiling reveals a function of the STN8 kinase in fine-tuning of cyclic electron flow (CEF). *Proc Natl Acad Sci USA* **108**: 12955–12960.

Rizhsky L, Liang H, Mittler R (2003). The water-water cycle is essential for chloroplast protection in the absence of stress. *J Biol Chem* **278**: 38921–38925.

Sakamoto H, Maruyama K, Sakuma Y, Meshi T, Iwabuchi M, Shinozaki K et al. (2004). Arabidopsis cys2/his2-type zinc-finger proteins function as transcription repressors under drought, cold, and high-salinity stress conditions. *Plant Physiol* **136**: 2734–2746.

Schmutz J, Cannon SB, Schlueter J, Ma J, Mitros T, Nelson W et al. (2010). Genome sequence of the palaeopolyploid soybean. *Nature* **463**: 178–183.

Szabo I, Bergantino E, Giacometti GM (2005). Light and oxygenic photosynthesis: energy dissipation as a protection mechanism against photo-oxidation. *EMBO Rep* **6**: 629–634.

Teramoto H, Nakamori A, Minagawa J, Ono TA (2002). Light-intensity-dependent expression of Lhc gene family encoding light-harvesting chlorophyll-a/b proteins of photosystem II in *Chlamydomonas reinhardtii*. *Plant Physiol* **130**: 325–333.

van Wijk KJ, van Hasselt PR (1993). Kinetic resolution of different recovery phases of photoinhibited photosystem II in cold-acclimated and non-acclimated spinach leaves. *Physiol Plantarum* **87**: 187–198.

Walters RG, Horton P (1991). Resolution of components of non-photochemical chlorophyll fluorescence quenching in barley leaves. *Photosynth Res* **27**: 121–133.

Wang P, Duan W, Takabayashi A, Endo T, Shikanai T, Ye J et al. (2006). Chloroplastic NAD(P)H dehydrogenase in tobacco leaves functions in alleviation of oxidative damage caused by temperature stress. *Plant Physiol* **141**: 465–474.

Warner DA, Edwards GE (1993). Effects of polyploidy on photosynthesis. *Photosynthesis Res* **35**: 135–147.

Wood TE, Takebayashi N, Barker MS, Mayrose I, Greenspoon PB, Rieseberg LH (2009). The frequency of polyploid speciation in vascular plants. *Proc Natl Acad Sci USA* **106**: 13875–13879.

Yamamoto HY, Kamite L (1972). The effects of dithiothreitol on violaxanthin de-epoxidation and absorbance changes in the 500-nm region. *Biochim Biophys Acta* **267**: 538–543.